ESRF

	Experiment title: Perylene-bismide self-assembled monolayers: internal order and thermal stability	Experiment number: MA-2078
Beamline: BM25B	**Date of experiment**: from: 12th December to: 18th DEcember	**Date of report**: 18/2/2014 revised report: 16/2/2015
Shifts: 18	**Local contact(s)**: Juan Rubio-Zuazo	*Received at ESRF:*

Names and affiliations of applicants (* indicates experimentalists):

* RESEL Roland, 11 December 2013 to 17 December 2013
* JONES Andrew, From:11 December 2013 to 19 December 2013
* CHATTOPADHYAY Basab,   11 December 2013 to 19 December 2013
* PACHMAJER Stefan,   11 December 2013 to 19 December 2013
* UNGER Katrin,   11 December 2013 to 19 December 2013
* EHMANN Heike   11 December 2013 to 19 December 2013

The suggested experiments could not be performed successfully, but two alternative experimental series gave good results:

H. M. Ehmann, O. Werzer,
Surface Mediated Structures: Stabilization of Metastable Polymorphs on the Example of Paracetamol
CRYSTAL GROWTH & DESIGN, vol. 14   iss. P. 3680-3684 (2014)

A. F. O. Jones, Y. Geerts, J. Karpinska, A. R. Kennedy, R. Resel, C. Rothel, C. Ruzie, O. Werzer, M. Sferrazza,
Substrate-induced phase of a [1]Benzothieno[3,2-b]benzothiophene derivative and phase evolution by aging and solvent vapor annealing.
ACS Applied Materials & Interfaces, vol. 7, iss. 3 p. 1868-73 (2015).

Report on the experimental performance on the original application

The beamtime application was originally formulated for beamline ID10-EH1. The experience with the set-up there was expected to be sucessful, since comparable measurements were already performed there. Although, the allocation of the beamline BM25B gave us the possibility to get insight into a new experimental facility with new possibilities, the alternative allocation cause some risk for a successful experimental performance. There is an excellent documentation of the beamline BM25B present at the homepage and several scientific publications on the performance of the beamlines are available, but the optimisation of the beamline is more in the field of inorganic materials.

In summary, the originally suggested experiment on self-assembled molecules did not work properly, but the two alternative projects gave excellent results.

beamline configuration:
height of the beam: 0.1 mm, vertical divergence of 0.25 mrd (= 0.14 deg)
width of the beam: 0.5 mm, horizontal divergence 2 mrd (= 0.11 deg)
wavelength: 0.9998 Angström, determined by Si-standard SRM 640C from NIST

The multi-purpose X-ray diffraction end-station was used together with the portable UHV/ambient pressure chamber. The thin film sample was mounted horizontally. The sample stage was covered by a cylindric Beryllium window to protected the organic film from degradation. A constant flow of Helium through the sample chamber was used.

Two detectors were used. A point detector was used for alignment of the sample relative to the primary beam, also for x-ray reflectivity and for specular diffraction. A two-dimensional CCD camera (photonic Science Ltd.) with a horizontal size of 250 mm and a vertical size of 83 mm (single pixel size of 62.5 µm x 62.5 µm) was used. The distance of the sample and the 2D-detector was 371.4 mm.

The critical angle of total external reflections was determined by x-ray reflectivity rocking curves using the position of the Yoneda peaks. A position of 0.14° deg was found for thermally oxidised silicon surfaces (most of the samples was on this surface). Finally an incidence angle of 0.13° was used for GIXD experiments. This angle is slightly below the critical angle of total external reflection, but it guarantees a penetration of the primary beam into the organic film but only weak penetration into the substrate material. Weak scatting singal from the substrate is expected. The position of the Yoneda poeak was regulary checked during the experiments

structure and thermal stability of self-assembled monolayers:

The synchrotron experiments were prepared by x-ray reflectivity studies perfomed with laboratory equipm,ent. Self-assembled monolayers of PBI-PA and PBIF-PA as well as of the spin coated monolayers of PBI-alkyl were studied. Even the thermal stabilities of these monolayers are determined by using laboratory equipment.

The starting point of the GIXD experiments at the synchrotron was the inverstigation of drop-casted films. These films are much thicker than monolayers, these films represent the bulk properties of the materials and not the monolayer structure. Figure 1 gives the GIXD pattern of a drop-casted PBI-alkyl film. The scattering from the organic material appears at low values of the scattering vector q ($q < 2A^{-1}$), while the background scattering of the set-up appears at larger q – values. The diffraction pattern shows quite well the expected features, e.g. a broad peak at $q = 1.8$ A^{-1} (d = 3.5 Angström) for the parallel stacking of the aromatic core of the molecule.

Unfortunately, no clear diffraction features could be obtained from the monolayer. The background of the experimental set-up is too high for the detection of a weakly ordered organic monolayer (compare Figure 2).

Similar results was obtained also for the two other self-assembled monolayers PBI-PA and PBIF-PA. While drop-casted films give a clear diffraction feature, monolayer does not give detectable intensities.
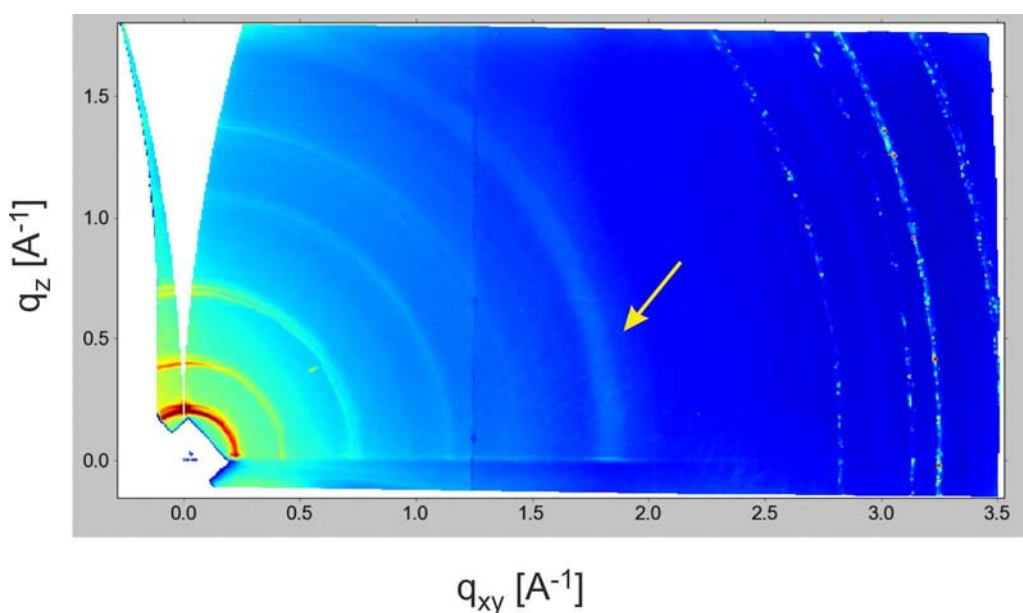
Figure 1: GIXD pattern of a drop-casted film of PBI-alkyl plotted as a reciprocal space map with q_{xy} as the in-plane part of the scattering vector and q_z the out-of-plane part of the scattering vector. The illumination time was 10 minutes. Diffraction features below $q = 2$ A^{-1} arise from the organic film, while diffraction features at large q-values are from the experimental set-up mainly from the beryllium window. The arrow gives the diffraction peak arising from the pi-pi stacking of the perylene units of the molecule.
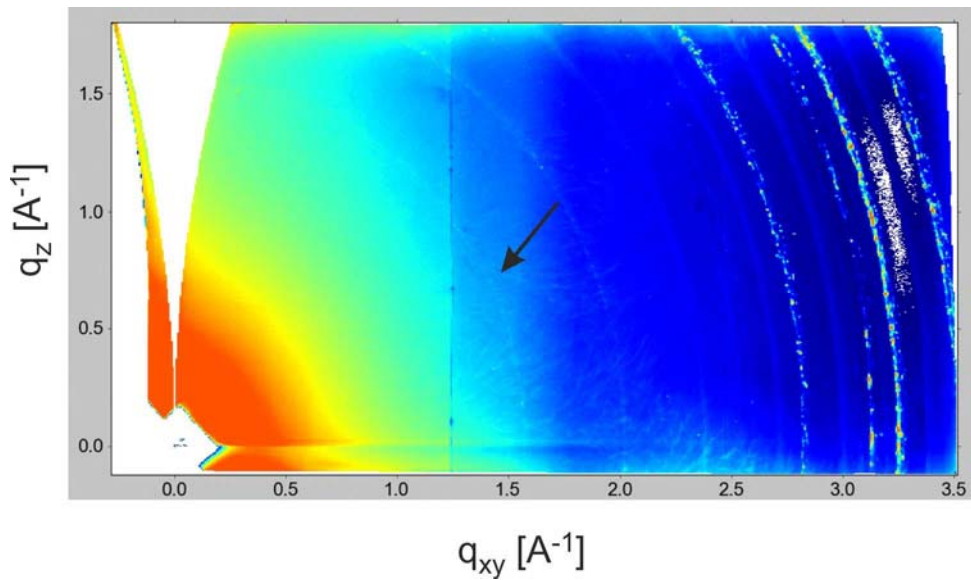
Figure 2: GIXD pattern of a spincoated monolayer of PBI-alkyl plotted as a reciprocal space map with qxy as the in-plane part of the scattering vector and qz the out-of-plane part of the scattering vector. The illumination time was 60 minutes. No clear diffraction feature of the monolayer could be detected, The sharp diffraction peak (marked with a black arrow) arises from the experimental set-up.

Surface Mediated Structures: Stabilization of Metastable Polymorphs on the Example of Paracetamol

Heike M. A. Ehmann* and Oliver Werzer

Institute of Pharmaceutical Science, Department of Pharmaceutical Technology, Karl-Franzens University of Graz, Universitätsplatz 1, 8010 Graz, Austria

Ⓢ Supporting Information

ABSTRACT: The preparation of typically thermodynamically unstable polymorphic structures is a challenge. However, solid surfaces are well established aids for the formation and stabilization of polymorphic structures within, for instance, organic electronics. In this study, we report the stabilization of a pharmaceutically relevant substance via a solid surface at ambient conditions. Form III of paracetamol, which is typically unstable in the bulk at standard conditions, can be stabilized with a model silica surface by a standard spin coating procedure followed by rapid heat treatment. Such a preparation technique allows the use of atomic force microscopy and grazing incidence X-ray diffraction measurements revealing detailed information on the morphology and structure of the polymorph. Furthermore, the results exhibit that this polymorph is stable over a long period of time revealing surface mediated stabilization. These findings demonstrate a novel approach to provide thermodynamic stability when applied to similar molecules with specific applications.
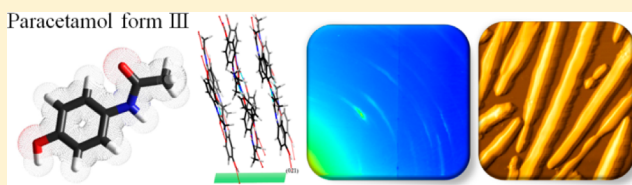
The controlled preparation of polymorphic structures and different crystal morphologies has become a hot topic in several research areas such as pharmaceutical technology,[1,2] crystal engineering,[3,4] organic electronics[5] as well as in material science.[6] Various polymorphs of a single substance differ by means of their physical and chemical properties such as solubility, bioavailability, morphology, crystal structure, or even thermodynamic stability.[7,8] Paracetamol, also known as acetaminophen (*N*-(4-hydroxyphenyl)acetamide), is widely used due to its antipyretic (fever depressant) and analgesic (painkiller) properties and is nowadays produced by many pharmaceutical companies at large scale.[9] The commercially utilized polymorph form I has a monoclinic crystal structure, which is not suitable for direct compression into tablets due to the lack of slipping planes which are necessary for plastic deformation.[10] In contrast, the orthorhombic paracetamol form II has well-defined slipping planes and undergoes plastic deformation upon compaction.[10] The crystallization behavior was studied intensively over the last decades, but nevertheless the elusive form III was recently characterized experimentally by means of its crystal structure.[11,12] A few procedures are known which describe the isolation and characterization of the thermodynamic less stable polymorph, e.g., nanoconfined in monoliths[13,14] or confined between glass slides[15] under the exclusion of air. It was shown that the confinement between glass slides is not necessary to isolate form III,[16] but the handling of the elusive polymorph in an air environment at standard conditions is still nowadays a challenge. These confined preparation conditions however lack the ability to use techniques such as atomic force microscopy (AFM) or grazing incidence X-ray diffraction (GIXD) to get further information on the morphology and structures within layers as thin as a couple of nanometers. It is known that surfaces are

able to induce specific polymorphs upon deposition.[5,17,18] Even the occurrence of surface mediated phases can be observed with distinct properties from the bulk.[5]

In this work, we describe different approaches to prepare paracetamol thin films containing defined polymorphs at a solid model surface. For this purpose, paracetamol was dissolved in ethanol (EtOH) or tetrahydrofuran (THF) and spin coated on precleaned thermally oxidized silicon wafers. The usage of silicon wafers as model substrates allow exclusion of roughness induced effects on the crystallization behavior. Both as-prepared samples result in completely amorphous films, followed by different crystallization kinetics and crystal morphologies. While the EtOH spin coated samples crystallized in a time frame of 24 h, the THF prepared samples revealed spherulitic crystallization induction after approximately 5 min. Compared to the literature,[16] the crystallization behavior in a confined environment is prolonged compared to crystallization at ambient conditions as it was done in this study (298 K, relative humidity 30%, 1 atm and under air). To prepare the elusive and thermodynamically unstable form III, a fresh and thus amorphous film was prepared from THF and was put in an oven at 383 K for 10 min without the exclusion of air. To provide optimal thermal contact, the oven was equilibrated whereby the fresh spun wafers were put on a heat-equilibrated alumina plate. The thermal conductivity of the used silicon wafer ensures fast thermal transfer, whereby the heat flow gradient is directed from the substrate toward the amorphous film. Variation in the preparation conditions showed that the
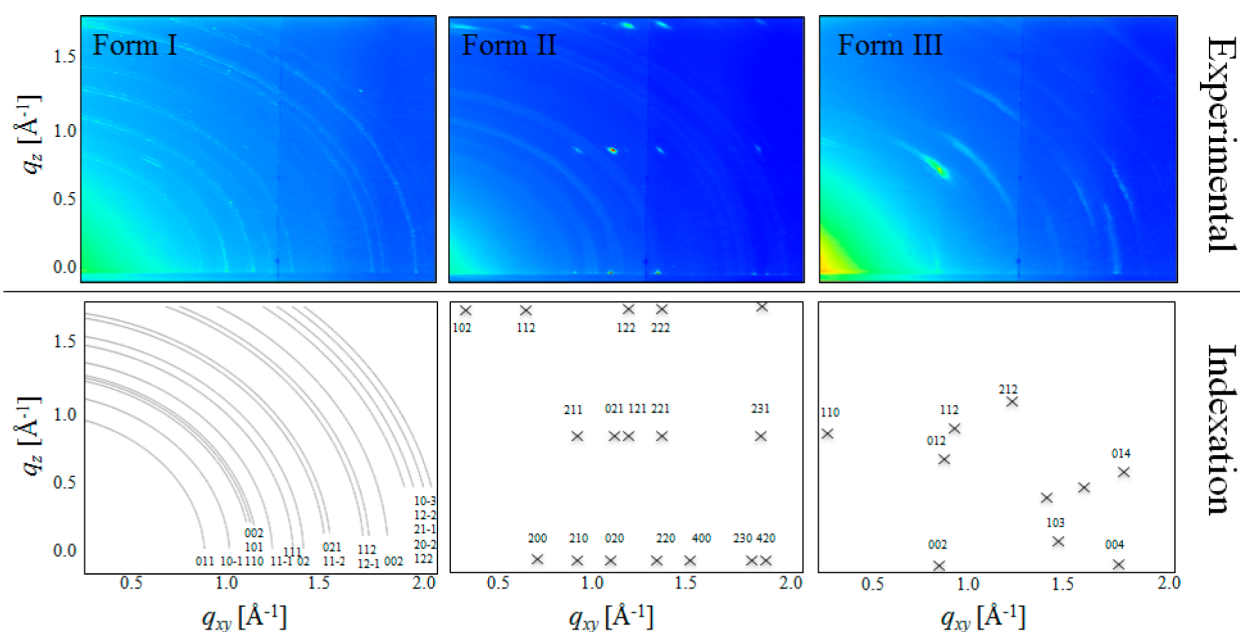
Figure 1. Experimental grazing incidence X-ray diffraction (GIXD; wavelength λ = 0.9998 Å; incidence angle α_i = 0.13°) patterns of all three polymorphs of paracetamol stabilized on SiO_x (upper row) with the corresponding theoretical indexation (lower row) with form I having a powder character and form II and form III having a 001 or 021, respectively, contact plane.

rapid temperature increase was necessary to obtain form III. This allows the assumption that the crystallization in the oven occurs at the hot solid substrate further allowing the thermodynamic unstable polymorph to be entrapped and stabilized at the silica substrate even without the exclusion of air. It is well-known in the literature that form III is unstable at ambient conditions under air and interconverts into form II and I.[16]

GIXD measurements of the three samples are shown in Figure 1. The GIXD measurement in general allows netplanes which are close to the surface-normal to be detected within thick films[19] (up to hundreds of nanometers for organic layers) as well as within thin films consisting of a monolayer.[20] High intensity spots correspond to Bragg reflections which can be used to index the pattern and thus to identify their crystal structures. The measurements of the sample containing form I reveal ring-like Bragg reflections showing that the crystallites arrange like a random oriented powder; i.e., no preferred orientation is observed. The indexation shows that all rings are a result of paracetamol being in the thermodynamic stable polymorph form I with a monoclinic unit cell (Figure 2). The GIXD pattern of form II shows defined spots at q_z = 0.0, 0.8, 1.7 nm^{-1} and various q_{xy}. The indexation reveals that these spots are a result of paracetamol being in form II conformation with an orthorhombic unit cell. In addition, the crystallites of form II show a preferred orientation with respect to the surface, whereby the 001 plane is in contact with the surface. However, rings are also present within the pattern indicating random oriented form I domains. This shows that the sample contains two polymorphs simultaneously, even if the amount of form I is very low compared to form II. The form III sample reveals a GIXD pattern with spots being distinct from the previously observed ones. The indexation of the spots can be achieved by introducing a 021 contact plane with respect to the surface with an orthorhombic unit cell (compare Figure 2). The smearing of the Bragg spots shows that the mosaicity of the crystalline needles is relatively high. This means that the molecules have a
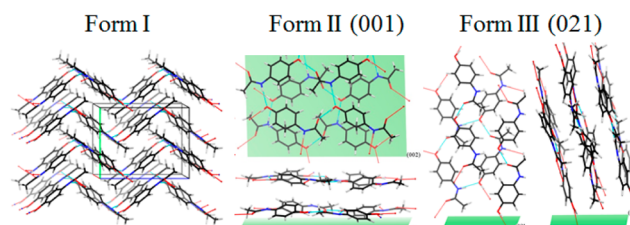
Polymorph	Form I	Form II	Form III
CSD code	HXACAN30	HXACAN08	HXACAN29
Temperature [K]	298	298	300
Space group	P2$_1$/a	Pbca	Pca2$_1$
a [Å]	7.01	17.17	11.84
b [Å]	9.21	11.78	8.56
c [Å]	11.60	7.21	14.82
β [°]	97.84	90.00	90.00

Figure 2. Visualization of the molecular arrangement within the crystal structures of paracetamol form I,[21] II,[21] and III[11] together with the contact plane with respect of the SiO_x surface. The table below summarizes the used crystal lattice parameters with their corresponding CSD code, space group, and corresponding temperature at which the experiments were performed.

certain degree of freedom to assemble at the silica surface which is different compared to form II with a nearly perfect alignment.

In Figure 2, the visualization of the three different crystal structures of the surface stabilized polymorphs is shown with the corresponding crystal structure parameters, which were used for indexation. Form I is shown in its typical herringbone packing of the paracetamol sheets, whereby the delocalized π-orbitals of the phenyl units are oriented toward the methyl groups of the next molecule. The intersheet assembling of the molecules is a result of H-bonding, while the intrasheet connection (sheet−sheet stacking) completely lacks any of

those. Form I is visualized with its monoclinic unit cell with no preferential alignment with respect to the surface due to its random orientation. The herringbone structure also is responsible for the mechanical stability and the disability for compaction required in tablet preparation.

In Figure 3 the morphologies of the three samples containing each polymorph of paracetamol at room temperature are shown
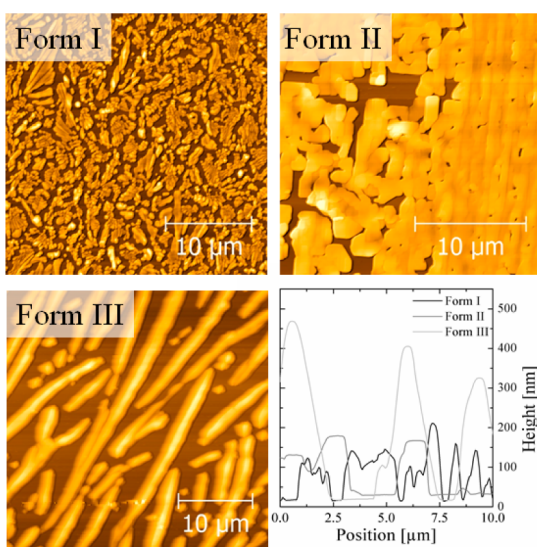
Figure 3. Atomic force microscopy height images of paracetamol form I, II, and III and the corresponding horizontal texture cuts taken in the middle of each image (lower right corner).

with their corresponding height profiles. The AFM image of form I reveals the typical shape of monoclinic crystals with prismatic to plate-like morphology, whereby the crystallites are randomly rotated with respect to each other. Form II shows a distinct growth morphology, and plate-like structures are present. While the crystal morphologies are distinct, the height and consequently the coverage are very similar to form I and II, showing that diffusion in the upward direction from the surface is negligible. These two observed morphologies fit very well to previously observed experiments on paracetamol, where morphological differences are explained by different growth faces being dominant.[22] The morphology of form III is distinct from the previous two forms, and needle-like structures are present. The coverage of the surface is strongly reduced, and consequently the heights of the needle-islands are higher compared to those of form I and II even though the nominal film thickness of the spin coated sample was very similar. The height of the needles is around 450 nm, which is about three times larger compared to the previous observed heights of form I and II.

Differences in the crystal structure and alignment are also reflected within their morphologies. The structure of form II is shown in a 001 orientation (Figure 2, green plane) which is parallel to the silica surface. This visualization reveals that the paracetamol molecules arrange in a way that maximizes their contact areas with the silicon surface. Further, the delocalized π-orbitals are slightly tilted toward the surface, but due to the large contact area, also the polar groups are in the highest possible contact to interact with the semipolar silica. Again intersheet H-bonds are visible, while intrasheet bonds of the hereby flatly arranged paracetamol sheets are not present (slipping plane of form II). According to the literature, form II

exhibits a plate-like growth whereby the slowest growing crystal face is the 001, which is in excellent agreement with our observations.[22] These findings indicate that growing into the a- and b-axis direction of the orthorhombic unit cell is equally likely and more favorable compared to the stacking into the c-axis direction. The arrangement of paracetamol molecules within the orthorhombic form III unit cell with respect to the 021 direction indicates that the molecules form hydrogen bonds toward the silicon surface and that the molecules stand nearly perpendicular to the substrate (Figure 2). Again the intersheet connection exhibits H-bonds, while the intrasheet stacking lacks any of those. The upright alignment of the form III sheets is in very good agreement with the observed needle-like morphology which was measured with AFM (Figure 3), whereby the paracetamol sheets seem to grow into the c-axis of the orthorhombic unit cell, or the molecules are perpendicular to the long needle axis. Further, the stability and reproducibility of the surface mediated stabilization of all three polymorphs of paracetamol was investigated. During the course of the synchrotron experiment, fresh prepared samples as well as 4-week-old samples were characterized revealing the same diffraction patterns. The samples were stored at ambient conditions (25 °C, relative humidity ~30%, 1 atm and under air environment), which reflects the potential of surface mediated stabilization. In addition, AFM investigations of the older samples did not reveal any significant change in the morphology, indicating that there is no rearrangement upon storage.

The surface mediated polymorph stabilization which was studied within this work using paracetamol is in excellent agreement with Ostwald's step rule which states that the least thermodynamic stable polymorph crystallizes first.[16] In particular, this means that a system moves to a thermodynamic equilibrium from an initial high energy state, whereby the least stable polymorph crystallizes first and rearranges stepwise into the different polymorphs (form III > form II > form I) due to changes within the free energy. Further, the different preparation conditions and the preferential alignment of the paracetamol molecules with respect to the surface indicate that the intensive (e.g., temperature, viscosity, chemical potential, density, etc.) and extensive (e.g., Gibbs free energy, entropy, mass, number of molecules, etc.) parameters of the solvent, analyte, and substrate in use are of crucial importance during surface mediated stabilization. EtOH exhibits a relatively low vapor pressure compared to THF. This suggests that EtOH solvent residues remain within the amorphous film, whereby molecule diffusion promotes the rearrangement in a thermodynamic stable configuration even if the viscosity of EtOH is about 2 times higher. Contrarily, the vapor pressure of THF is about 3 times larger compared to EtOH at standard conditions, meaning that THF molecules evaporate fast allowing the thermodynamic metastable polymorph II to be stabilized at the silica surface at 298 K. A shorter time frame typically means that formation of a thermodynamically less stable form is favored in accordance with other literature reports.[23,24] The unstable forms II and III most likely develop due to the fast processing condition within the THF solutions. A rapid temperature increase to 383 K of an amorphous paracetamol film spin coated from THF results in polymorph III being stabilized at the silica surface. An increase in temperature typically reduces the H-bonding interaction strength which reduces the affinity for the molecules to interact with the substrate. Furthermore, higher temperatures mean that the

molecules require more space on account of molecular vibration. Both effects favor the formation of upright standing molecules on top of the substrate surface which in the case of paracetamol means additionally assembling into form III.

By comparing the observed alignment of paracetamol form III with different literature statements, it can be seen that the orientation of form III crystallites is highly influenced by the surface in use even if different preparation methods indicate similar growth kinetics of form III. In a recent publication,[25] the authors state that form III, when confined in self-ordered anodic aluminum oxide nano tubes (AAO), preferentially crystallizes with its 001 plane being parallel to the AAO interface. This alignment indicates that no H-bonds are formed between the AAO host and the paracetamol molecules. Contrarily, our investigations strongly indicate the formation of H-bonds between the semipolar silica substrate and the paracetamol molecules with the 021 reflection plane being parallel to the surface. The differences in the preparation method aside, this direct comparison indicates the strong influence of the surface energetic properties of the surfaces in use; i.e., variation of the surface induces a distinct growth behavior. A previous work[26] suggested that along the a-axis of paracetamol only short-range order is present, which also corresponds to the slowest growth direction in the calculated morphology of form III.[22] This is in excellent agreement with the observed morphology of paracetamol form III revealing preferential growth in the needle axis of the c-direction of the orthorhombic unit cell.

■ ASSOCIATED CONTENT

ⓢ Supporting Information
Experimental details. This material is available free of charge via the Internet at http://pubs.acs.org.

■ AUTHOR INFORMATION

Corresponding Author
*E-mail: heike.ehmann@uni-graz.at; phone: 00433163808291.

Notes
The authors declare no competing financial interest.

■ ACKNOWLEDGMENTS

■ REFERENCES

(1) Werzer, O.; Kunert, B.; Roblegg, E.; Zimmer, A.; Oehzelt, M.; Resel, R. Surface Induced Order of Solution Processed Caffeine Needles on Silica and Muscovite Mica. *Cryst. Growth Des.* **2013**, *13* (3), 1322−1328.

(2) Neumann, M. A.; Perrin, M.-A. Can crystal structure prediction guide experimentalists to a new polymorph of paracetamol? *CrystEngComm* **2009**, *11* (11), 2475−2479.

(3) Blagden, N.; de Matas, M.; Gavan, P. T.; York, P. Crystal engineering of active pharmaceutical ingredients to improve solubility and dissolution rates. *Adv. Drug Delivery Rev.* **2007**, *59* (7), 617−630.

(4) Lee, T.; Hung, S. T.; Kuo, C. S. Polymorph farming of acetaminophen and sulfathiazole on a chip. *Pharm. Res.* **2006**, *23* (11), 2542−2555.

(5) Werzer, O.; Boucher, N.; de Silva, J. P.; Gbabode, G.; Geerts, Y. H.; Konovalov, O.; Moser, A.; Novak, J.; Resel, R.; Sferrazza, M. Interface induced crystal structures of Dioctyl-Terthiophene thin films. *Langmuir* **2012**, *28* (22), 8530−8536.

(6) Thankaraj Salammal, S.; Balandier, J.-Y.; Arlin, J.-B.; Olivier, Y.; Lemaur, V.; Wang, L.; Beljonne, D.; Cornil, J.; Kennedy, A. R.; Geerts, Y. H. Polymorphism in Bulk and Thin Films: The Curious Case of Dithiophene-DPP (Boc)-Dithiophene. *J. Phys. Chem. C* **2014**, *118*, 657−669.

(7) Rodríguez-Spong, B.; Price, C. P.; Jayasankar, A.; Matzger, A. J.; Rodríguez-Hornedo, N. r. General principles of pharmaceutical solid polymorphism: A supramolecular perspective. *Adv. Drug Delivery Rev.* **2004**, *56* (3), 241−274.

(8) Desiraju, G. R. Crystal Engineering: From Molecule to Crystal. *J. Am. Chem. Soc.* **2013**, *135*, 9952−9967.

(9) Beames, J. M.; Hudson, A. J. Jet-cooled spectroscopy of paracetamol. *Phys. Chem. Chem. Phys.* **2010**, *12* (16), 4157−4164.

(10) André, V.; da Piedade, M. F. M.; Duarte, M. T. Revisiting paracetamol in a quest for new co-crystals. *CrystEngComm* **2012**, *14* (15), 5005−5014.

(11) Perrin, M. A.; Neumann, M. A.; Elmaleh, H.; Zaske, L. Crystal structure determination of the elusive paracetamol Form III. *Chem. Commun. (Cambridge)* **2009**, *22*, 3181−3.

(12) Gaisford, S.; Buanz, A. B.; Jethwa, N. Characterisation of paracetamol form III with rapid-heating DSC. *J. Pharm. Biomed. Anal.* **2010**, *53* (3), 366−70.

(13) Beiner, M.; Rengarajan, G.; Pankaj, S.; Enke, D.; Steinhart, M. Manipulating the crystalline state of pharmaceuticals by nanoconfinement. *Nano Lett.* **2007**, *7* (5), 1381−1385.

(14) Rengarajan, G.; Enke, D.; Steinhart, M.; Beiner, M. Size-dependent growth of polymorphs in nanopores and Ostwald's step rule of stages. *Phys. Chem. Chem. Phys.* **2011**, *13* (48), 21367−21374.

(15) Di Martino, P.; Conflant, P.; Drache, M.; Huvenne, J.-P.; Guyot-Hermann, A.-M. Preparation and physical characterization of forms II and III of paracetamol. *J. Therm. Anal. Calorim.* **1997**, *48* (3), 447−458.

(16) Burley, J. C.; Duer, M. J.; Stein, R. S.; Vrcelj, R. M. Enforcing Ostwald's rule of stages: Isolation of paracetamol forms III and II. *Eur. J. Pharm. Sci.* **2007**, *31* (5), 271−276.

(17) Werzer, O.; Stadlober, B.; Haase, A.; Flesch, H. G.; Resel, R. Evaluation of organic sub-monolayers by X-ray based measurements under gracing incident conditions. *Eur. Phys. J. Appl. Phys.* **2009**, *46* (2), DOI: 10.1051/epjap/2009038.

(18) Werzer, O.; Stadlober, B.; Haase, A.; Oehzelt, M.; Resel, R. Full X-ray pattern analysis of vacuum deposited pentacene thin films. *Eur. Phys. J. B* **2008**, *66* (4), 455−459.

(19) Moser, A.; Novak, J.; Flesch, H.-G.; Djuric, T.; Werzer, O.; Haase, A.; Resel, R. Temperature stability of the pentacene thin-film phase. *Appl. Phys. Lett.* **2011**, *99* (22), 221911−221911−3.

(20) Smits, E. C.; Mathijssen, S. G.; Van Hal, P. A.; Setayesh, S.; Geuns, T. C.; Mutsaers, K. A.; Cantatore, E.; Wondergem, H. J.; Werzer, O.; Resel, R. Bottom-up organic integrated circuits. *Nature* **2008**, *455* (7215), 956−959.

(21) Nichols, G.; Frampton, C. S. Physicochemical characterization of the orthorhombic polymorph of paracetamol crystallized from solution. *J. Pharm. Sci.* **1998**, *87* (6), 684−693.

(22) Beyer, T.; Day, G. M.; Price, S. L. The prediction, morphology, and mechanical properties of the polymorphs of paracetamol. *J. Am. Chem. Soc.* **2001**, *123* (21), 5086−5094.

(23) Wedl, B.; Resel, R.; Leising, G.; Kunert, B.; Salzmann, I.; Oehzelt, M.; Koch, N.; Vollmer, A.; Duhm, S.; Werzer, O. Crystallisation kinetics in thin films of dihexyl-terthiophene: the appearance of polymorphic phases. *RSC Adv.* **2012**, *2* (10), 4404−4414.

(24) Lercher, C.; Resel, R.; Balandier, J.-Y.; Niebel, C.; Geerts, Y. H.; Sferrazza, M.; Gbabode, G. Effects of temperature on the polymorphism of α, ω-dioctylterthiophene in thin films. *J. Cryst. Growth* **2014**, *386*, 128−134.

(25) Graubner, G.; Rengarajan, G. T.; Anders, N.; Sonnenberger, N.; Enke, D.; Beiner, M.; Steinhart, M. Morphology of porous hosts directs preferred polymorph formation and influences kinetics of solid/solid transitions of confined pharmaceuticals. *Cryst. Growth Des.* **2013**, *14* (1), 78−86.

(26) Peterson, M. L.; Morissette, S. L.; McNulty, C.; Goldsweig, A.; Shaw, P.; LeQuesne, M.; Monagle, J.; Encina, N.; Marchionna, J.; Johnson, A. Iterative high-throughput polymorphism studies on acetaminophen and an experimentally derived structure for form III. *J. Am. Chem. Soc.* **2002**, *124* (37), 10958−10959.

(27) Hammersley, A. P. *FIT2D V9.129 Reference Manual V3.1*; ESRF: Grenoble, 1998.

(28) Hammersley, A. P. *FIT2D: An Introduction and Overview*; ESRF: Grenoble, 1997.

(29) Hammersley, A.; Svensson, S.; Hanfland, M.; Fitch, A.; Hausermann, D. Two-dimensional detector software: from real detector to idealised image or two-theta scan. *Int. J. High Pressure Res.* **1996**, *14* (4−6), 235−248.

(30) Hammersley, A. P.; Svennson, S. O.; Thompson, A. Calibration and correction of spatial distortions in 2D detector systems1994.

(31) Moser, A.; Werzer, O.; Flesch, H.-G.; Koini, M.; Smilgies, D.-M.; Nabok, D.; Puschnig, P.; Ambrosch-Draxl, C.; Schiek, M.; Rubahn, H.-G. Crystal structure determination from two-dimensional powders: A combined experimental and theoretical approach. *Eur. Phys. J. Spec. Top.* **2009**, *167* (1), 59−65.

Substrate-Induced Phase of a [1]Benzothieno[3,2-*b*]benzothiophene Derivative and Phase Evolution by Aging and Solvent Vapor Annealing

Andrew O. F. Jones,*,† Yves H. Geerts,‡ Jolanta Karpinska,‡ Alan R. Kennedy,‖ Roland Resel,§ Christian Röthel,§ Christian Ruzié,‡ Oliver Werzer,¶ and Michele Sferrazza†

†Département de Physique, Faculté des Sciences, Université Libre de Bruxelles CP223, Campus de la Plaine, 1050 Brussels, Belgium
‡Laboratoire de Chimie des Polymères, Faculté des Sciences, Université Libre de Bruxelles CP206/01, Campus de la Plaine, 1050 Brussels, Belgium
‖Department of Pure and Applied Chemistry, University of Strathclyde, 295 Cathedral Street, Glasgow G1 1XL, Scotland
§Institute of Solid State Physics, Graz University of Technology, Petersgasse 16, 8010 Graz, Austria
¶Institute of Pharmaceutical Sciences, Department of Pharmaceutical Technology, Karl-Franzens Universität Graz, Universitätsplatz 1, 8010 Graz, Austria

Ⓢ Supporting Information

ABSTRACT: Substrate-induced phases (SIPs) are polymorphic phases that are found in thin films of a material and are different from the single crystal or "bulk" structure of a material. In this work, we investigate the presence of a SIP in the family of [1]benzothieno[3,2-*b*]benzothiophene (BTBT) organic semiconductors and the effect of aging and solvent vapor annealing on the film structure. Through extensive X-ray structural investigations of spin coated films, we find a SIP with a significantly different structure to that found in single crystals of the same material forms; the SIP has a herringbone motif while single crystals display layered $\pi-\pi$ stacking. Over time, the structure of the film is found to slowly convert to the single crystal structure. Solvent vapor annealing initiates the same structural evolution process but at a greatly increased rate, and near complete conversion can be achieved in a short period of time. As properties such as charge transport capability are determined by the molecular structure, this work highlights the importance of understanding and controlling the structure of organic semiconductor films and presents a simple method to control the film structure by solvent vapor annealing.

KEYWORDS: organic electronics, X-ray diffraction, substrate-induced phase, polymorphism, organic thin films
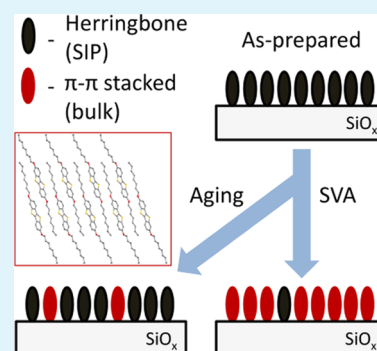
INTRODUCTION

In the field of organic electronics, the dependence of charge-transport capabilities on molecular structure is well-established and consideration of the semiconductor molecular structure is a key aspect in the optimal design of organic field-effect transistors (OFETs).[1−4] As the majority of charge transport occurs within the first few molecular layers, knowledge and control of the molecular structure at the substrate−film interface is therefore of great importance when considering materials for OFETs.[5] It has been demonstrated that the structure close to the substrate is not always the same as that of the bulk and so-called thin film, surface-mediated, or substrate-induced phases (SIPs) may form.[6,7] These polymorphic phases, which are typically not found as single-crystal structures, were first observed in films of the prototypical organic semiconductor pentacene,[8−13] and have since been found in other systems.[14−20] In films of pentacene, the SIP is found to be less energetically favorable than the bulk phase in isolation, but is stabilized close to the substrate because of improved compatibility of the structure with the flat surface of the

substrate, such that in the presence of the substrate it is the most stable form.[21,22] The structural difference between the SIPs and bulk phases of π-conjugated molecules is most often related to a small change in the tilt angle between the approximately upright-standing molecules and the substrate, resulting in more favorable molecule−substrate interactions and a decrease in the out-of-plane lattice spacing such that the two phases are similar but distinct from one another.[13,23,24] Moreover, SIPs are found to be present only up to a certain film thickness, after which the bulk form grows on top so that two phases coexist within a thick film.[15,23−25] It is therefore clear that the structure of the SIP may influence charge mobility and potential device performance when present due to its proximity to the substrate.

For solution-processed OFETs, other considerations are the various secondary effects (e.g., rapid solvent evaporation,

dewetting, etc.) which occur during coating and impact on the long-range molecular order.[26,27] This has led to the routine treatment of films postcoating, with a view to improving molecular ordering; thermal annealing, and more recently solvent vapor annealing (SVA),[28] are two examples of processes which may be utilized. The sometimes high temperatures required for thermal annealing can limit the choice of substrate and the choice of semiconducting material because of melting or thermal decomposition; this makes SVA an attractive proposition, as it is less harsh on the sensitive systems used in organic electronics. Furthermore, it has been demonstrated that use of a SVA processing step can lead to improved device performance when compared with using thermal annealing alone.[29] When applied to pentacene films displaying a SIP, thermal annealing or SVA initiates a conversion to the bulk form.[7,30,31] This shows further potential for annealing to not only increase long-range order but also to lead to a reorganization of molecules and potentially alter film properties significantly.

In this work, we investigate the possible presence of a SIP in films of a symmetrically alkylated [1]benzothieno[3,2-b]-benzothiophene (BTBT) derivative and the effect of time and SVA on the stability or evolution of the crystalline structure and morphology. Alkylated BTBT derivatives have shown great potential for use in air-stable, high performance, solution-processable OFETs.[32−38] Charge transport mobilities of up to 3.5 cm^2 V^{-1} s^{-1} have been recorded for polycrystalline films of dioctyl-BTBT (C_8−BTBT-C_8),[34] with even higher values recorded for single crystals.[35,39] Modification of the alkyl chain length of symmetrically substituted BTBT cores does not alter the arrangement of these BTBT cores; symmetrically dialkylated derivatives are isostructural with a herringbone (HB) packing motif and no SIPs are currently known for this class of molecule.[33] The subject of this study, dioctyloxy-BTBT (C_8O-BTBT-OC_8) (Figure 1), has an oxygen atom added
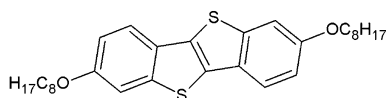
Figure 1. Molecular structure of C_8O-BTBT-OC_8.

between the BTBT core and the alkyl chains to encourage a different packing motif;[40] we will investigate whether this structural change leads to the presence of a SIP, using a variety of techniques to determine the solid-state arrangement of molecules in spin-coated films.

EXPERIMENTAL SECTION

Synthesis of C_8O-BTBT-OC_8 is detailed in the Supporting Information.

Crystal Structure. Single crystals of C_8O-BTBT-OC_8 were grown by slow evaporation of unsaturated HPLC grade hexane solutions. X-ray diffraction data for crystals of the compound were collected at 123 K with graphite monochromated Mo Kα radiation (λ = 0.71073 Å) using an Oxford Diffraction Xcalibur E instrument. All non-hydrogen atoms were refined anisotropically. Hydrogen atoms were included in calculated positions utilizing riding modes. The structure was refined to convergence using all unique reflections and against F^2 with the SHELXL-97 program.[41] $C_{30}H_{40}O_2S_2$, M_r = 496.74, triclinic, space group $P\bar{1}$, a = 5.5225(4), b = 8.0712(4), c = 31.0578(15) Å, α = 94.482(4), β = 92.994(5), γ = 105.696(5)°, V = 1324.76(13) Å^3, Z = 2, μ = 0.226 mm^{-1}; $2\theta_{max}$ = 54.0°, 10939 reflections, 5633 unique, R_{int} = 0.0474; final refinement to convergence on F^2 gave R = 0.0537 (F,

4012 obs. data only) and R_w = 0.1040 (F^2, all data), GOF = 1.054. Detailed crystallographic data with refinement parameters are listed in complete crystallographic information files (CIF).

Polarized Optical Microscopy. Films were studied with a Nikon Eclipse E200 microscope equipped with a Nikon DS-Fi1 digital camera. Images were treated using the NIS-Elements software package (version 3.0).

Atomic Force Microscopy (AFM). Measurements were performed using a Nanosurf Easyscan 2 instrument in noncontact mode. A TAP 190 cantilever (Budgetsensors) with a nominal resonance frequency of 190 kHz was used. Data analysis and visualization were performed using the Gwyddion software package.[42]

Thin Film Preparation. Samples were prepared on silicon wafers (SIEGET WAFER Gmbh) with a 150 nm thick thermally grown oxide layer (SiO$_x$). Substrates were cleaned in an ultrasonic bath in acetone for 15 min and then isopropanol for a further 15 min, before drying with CO$_2$ gas. Films were prepared by spin-coating from chloroform solutions (150 μL, 10.8 mg mL^{-1}) at a rotation speed of 2500 rpm for 45s. Solutions were filtered through a 0.2 μL PTFE syringe filter immediately before film deposition. Films were solvent vapor annealed by placing the spin-coated film in a sealed glass beaker with chloroform solvent (50 mL) for 6 days.

X-ray Measurements. Specular X-ray diffraction (sXRD) measurements were performed on a PANalytical EMPYREAN reflectometer setup equipped with a copper sealed tube, a 1/32° primary slit, 10 mm beam mask and a multilayer mirror (λ = 1.54 Å) on the primary side. A receiving slit of 0.1 mm and a 3D PANalytical PIXcel detector were used on the secondary side. Grazing incidence X-ray diffraction (GIXD) measurements were performed at the BM25b beamline[43] at the ESRF (Grenoble, France) using X-rays with a wavelength of 0.9998 Å and an incident angle of α_i = 0.13°, just below the critical angle of the substrate. The sample was placed in a beryllium chamber[44] and data were collected under an N$_2$ gas flow. Diffracted intensities were measured using a 2D CCD area detector (Photonic Science Ltd.). Data were converted to reciprocal space maps using the in-house-developed software package PyGID, which was also used for peak indexation.[45] Additional GIXD measurements were conducted at BESSY II (Berlin, Germany) at the KMC-2 beamline using X-rays with a wavelength of 1.00 Å and a 2D cross-wire detector (BRUKER).[46] An incident angle of α_i = 0.13° was chosen to enhance the scattered intensities. To minimize the beam damage of the samples, we directly applied a constant flow of argon on the samples. The reciprocal space maps were calculated with the *xrayutilities* library for Python.[47]

RESULTS AND DISCUSSION

The single-crystal structure of C_8O-BTBT-OC_8 is shown in Figure 2 and the unit-cell parameters are displayed in Table 1. The structure is found to be layered, with slipped π−π stacking of the molecular cores and an interdigitation of molecules, in contrast to the HB motif displayed by other dialkylated BTBT derivatives (the unit-cell parameters of C_8-BTBT-C_8 are listed in Table 1).[33] This interdigitated structure could intuitively lead to an incompatibility with a flat surface so that, as in the case of pentacene, a different structure may form in the presence of a surface because of this incompatibility.[13,23,24]

C_8O-BTBT-OC_8 films were spin-coated from chloroform solution onto precleaned silicon wafers with a 150 nm layer of thermally grown oxide. AFM measurements (Figure 3a) and optical microscopy (see the Supporting Information) show that the as-prepared polycrystalline films are very rough with many individual crystallites visible; AFM measurements show a film thickness of approximately 65 nm with an average roughness of 18 nm. This thickness suggests the film is approximately 22 molecular layers thick, if molecules are standing upright with the long molecular axis perpendicular to the substrate (molecular length of 33.88 Å), as is commonly the case for films of rodlike conjugated molecules.[48]
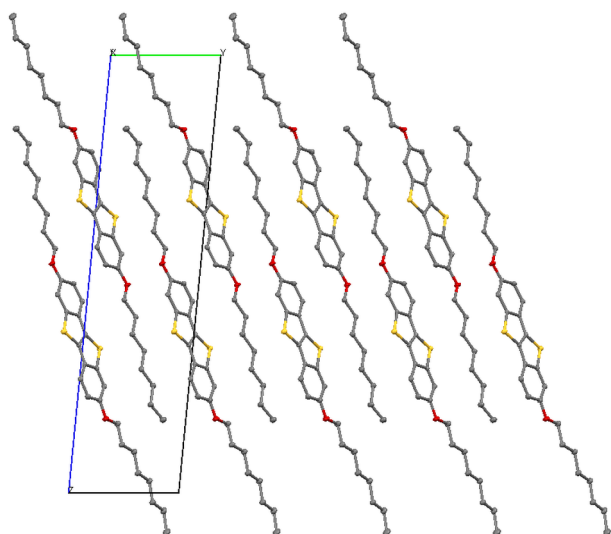
Figure 2. Single-crystal structure of C_8O-BTBT-OC_8 showing the unit cell and interdigitation of molecules. Hydrogen atoms have been removed for clarity.

Specular X-ray diffraction (sXRD) measurements, which measure only the lattice spacing perpendicular to the plane of the substrate, show several diffraction peaks (Figure 3c). The 001 reflection is observed at $q_z = 0.20$ Å^{-1}, along with higher order reflections, giving an out-of-plane lattice spacing of 30.85 Å. This is comparable to the 31.06 Å of the 001 of the bulk single-crystal structure but distinct; the d-spacing of 30.85 Å is close to the molecular length (33.88 Å) suggesting upright-standing molecules are present. This is very similar to other examples of SIPs such as pentacene, where only small changes in the out-of-plane lattice spacings occur even though a new molecular arrangement exists.[49]

Grazing incidence X-ray diffraction (GIXD) measurements were carried out to investigate the in-plane structure, i.e., the periodic packing within a sheet of C_8O-BTBT-OC_8, and the results show that the structure is in fact very different to that of the bulk. Films were first measured at the ESRF in Grenoble, France, and the same samples were then measured again 6 months later at BESSY II in Berlin, Germany. Peaks are observed along rods at $q_{xy} = 1.34$, 1.64, and 1.95 Å^{-1} at various q_z; none of these peaks should be present from the bulk structure and no other peaks are observed, showing a SIP has formed (Figure 4, left). The broadness of the peaks suggests that the crystalline domains are small. Using the unit cell of the known C_8−BTBT-C_8 structure (Table 1) as a starting point,[33] all diffraction peaks can be indexed by a slight adjustment of all unit cell parameters of this known structure; a monoclinic unit cell with two molecules in the asymmetric unit is able to explain the experimental GIXD pattern (Figure 4 and Table 1). The similarity of this unit cell to those of other dialkylated BTBT derivatives suggests that the SIP of C_8O-BTBT-OC_8 has

molecules in a HB packing formation, in contrast to the layered, slipped π−π stacked structure observed in the bulk. Close packing is accepted to be the main driver in crystal structure formation and, therefore, the fact that the SIP is found to be less dense than the bulk structure (Table 1) may suggest that the SIP is a metastable form induced by the substrate.[50] It has not been possible to determine the exact HB angle or angle of tilt from the from these X-ray measurements, however, the strength of 020 reflection suggests that the BTBT cores (as the most electron dense fragments) are aligned approximately parallel to the a-axis in the 020 plane and that the difference between the out-of-plane lattice spacing and the molecular length likely arises from the alkyl chains bending away from the BTBT cores toward the substrate as opposed to a tilting of the core itself.

The measurements conducted 6 months later show a similar diffraction pattern, however, now with the addition of new peaks (Figure 4, middle). The SIP is still the dominant phase, while new peaks are visible at $q_{xy} = 0.82$, 1.16, and 1.66 Å^{-1} at various q_z. These new peaks can be assigned to the bulk structure and show an evolution from a metastable SIP toward the bulk has occurred over time. It is unclear if over a longer period of time the complete structure would convert to the bulk (including at the interface with the dielectric); even a slight conversion between forms could have a significant impact on the electronic properties and further underlines the importance of identifying and understanding SIPs.

With the presence of the SIP established, the effect of SVA on the film morphology and structure was investigated. Films were solvent annealed for 6 days using chloroform vapor. Long annealing times were chosen to ensure that samples had fully undergone any changes arising from the SVA process. AFM (Figure 3b) and optical microscopy (see the Supporting Information) measurements show significant changes to the film morphology. Larger domains of a regular shape are now present with a lower surface coverage and exposed (molecule free) substrate. sXRD measurements (Figure 3c) show only a small change in the out-of-plane structure (lattice spacing of 31.10 Å), whereas sharper diffraction peaks and the regular shape of domains indicate improved film crystallinity.

GIXD measurements after SVA reveal a large number of new peaks. Many of these peaks are affected by splitting, making interpretation of the data more difficult. Despite this difficulty, it is clear that the bulk structure dominates and peaks at 0.82, 1.18, 1.58, and 1.66 Å^{-1} in q_{xy} can be indexed with the bulk unit cell (Table 1 and Figure 4, right). This shows that the SVA process has induced a conversion from the SIP to the bulk phase, effectively the same process which occurs due to aging but at a significantly increased rate. The conversion may, however, not be complete and peaks at 1.62 Å^{-1} in q_{xy} could correspond to the bulk or the SIP. There are also peaks present at 1.20 and 1.54 Å^{-1} in q_{xy} that cannot be indexed using the two, now known, structures of C_8O-BTBT-OC_8. These peaks

Table 1. Unit-Cell Parameters of the Different Crystal Phases of C_8O-BTBT-OC_8 and the Related C_8-BTBT-C_8

sample	a (Å)	b (Å)	c (Å)	α (deg)	β (deg)	γ (deg)	ρ (g cm^{-3})
C_8O-BTBT-OC_8 Single X-tal[a]	5.5225(4)	8.0712(4)	31.058(2)	94.482(4)	92.994(5)	105.696(5)	1.245
C_8O-BTBT-OC_8 Bulk SVA[b]	5.56	8.27	30.89	96.50	93.00	107.80	1.233
C_8O-BTBT-OC_8 SIP	6.02	7.75	31.08	90	97.00	90	1.146
C_8−BTBT-C_8[33]	5.927(7)	7.88(1)	29.18(4)	90	92.443(4)	90	1.133

[a]Single-crystal data collected at 123 K. [b]Film measured at room temperature.
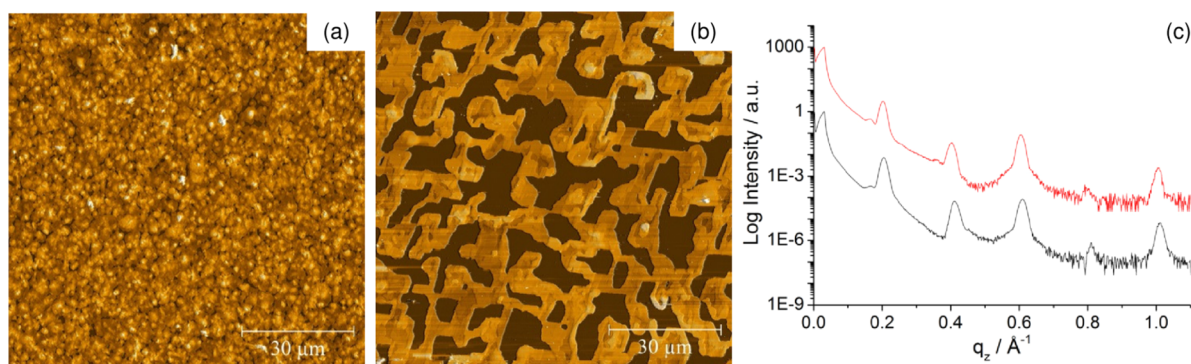
Figure 3. AFM images of (a) as-prepared and (b) solvent-annealed films and (c) sXRD patterns of the same as-prepared (black) and solvent annealed (red) films.
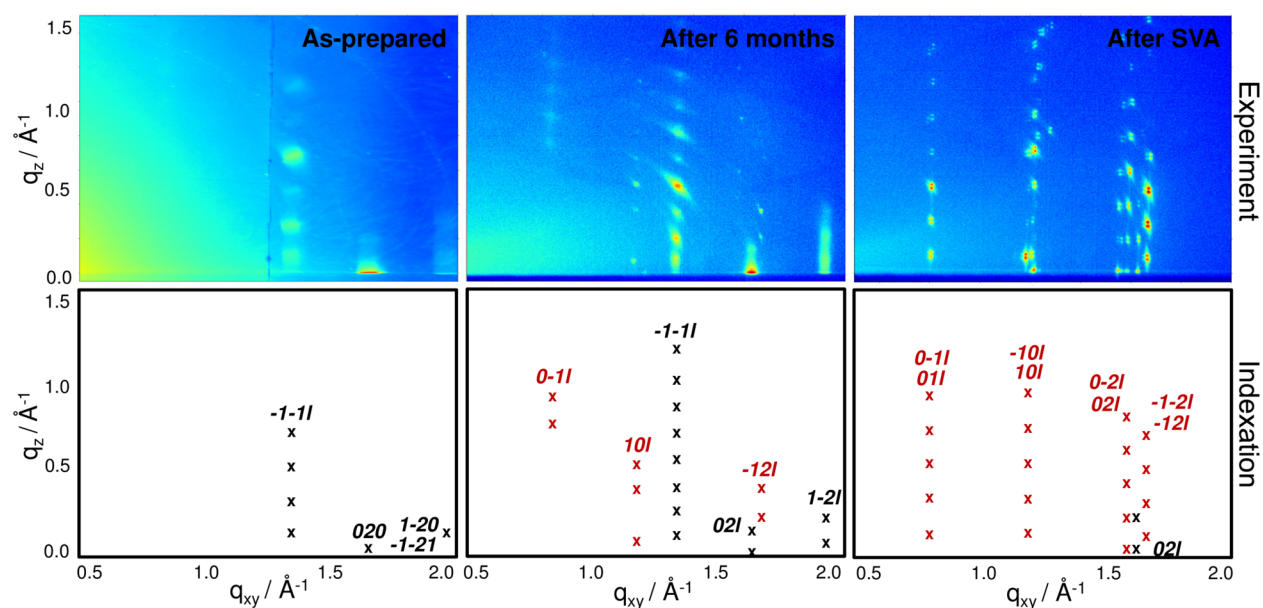
Figure 4. Experimental GIXD patterns of C_8O-BTBT-OC_8 films (above) and the corresponding peak indexation (below). Black crosses show peaks belonging to the SIP, whereas red crosses belong to the bulk phase.

could arise from a third, unknown, polymorphic phase or they could be the result of a supercell of either the SIP or the bulk phase, as a doubling of the in-plane lattice parameters of either phase can then account for these peaks and was also observed for a similar system previously.[15]

Films were also prepared from *o*-xylene solutions using the same preparation parameters (solution concentration, spin-coating speed, etc.). Optical microscopy, AFM, sXRD, and GIXD data are presented in the Supporting Information. The films display the same behavior as those described above, with a SIP transforming into the bulk by long time aging and more rapidly by SVA. This shows that, in the case of C_8O-BTBT-OC_8 on silica, the choice of solvent during preparation does not have an effect on the crystal structure of resultant films, and an SIP still forms regardless.

■ CONCLUSIONS

In conclusion, we have presented a detailed structural investigation of spin-coated films of C_8O-BTBT-OC_8 on a solid silica surface. A SIP with a HB packing motif is formed, in contrast to the slipped $\pi-\pi$ stacking of the bulk, and the same structure persists regardless of the solvent used during sample preparation. Over 6 months, the SIP structure slowly evolves

toward that of the bulk. Using SVA, the rate of conversion to the bulk can be greatly increased and gives almost complete conversion within a few days, providing a simple method to switch from the SIP to the bulk polymorph. Furthermore, this is the first example of a SIP that has a completely different packing arrangement from that of the bulk and is not only related to a change in the molecular tilt of the core typically responsible for the charge transport. This work emphasizes the importance of SIPs when dealing with organic electronics and shows the potential for SVA to be used for polymorph selection.

■ ASSOCIATED CONTENT

ⓢ Supporting Information

Synthesis of C_8O-BTBT-OC_8. Crystallographic information file for C_8O-BTBT-OC_8. Optical microscopy data of films produced from chloroform solution. Optical microscopy, AFM, sXRD, and GIXD data of films produced from *o*-xylene solutions. This material is available free of charge via the Internet at http://pubs.acs.org.

■ AUTHOR INFORMATION

Corresponding Author
*E-mail: andrew.jones@tugraz.at.

Notes
The authors declare no competing financial interest.

■ REFERENCES

(1) Dinelli, F.; Murgia, M.; Levy, P.; Cavallini, M.; Biscarini, F.; de Leeuw, D. M. Spatially Correlated Charge Transport in Organic Thin Film Transistors. *Phys. Rev. Lett.* **2004**, *92*, 116802.

(2) Coropceanu, V.; Cornil, J.; da Silva Filho, D. A.; Olivier, Y.; Silbey, R.; Brédas, J.-L. Charge Transport in Organic Semiconductors. *Chem. Rev.* **2007**, *107*, 926−952.

(3) Mas-Torrent, M.; Rovira, C. Role of Molecular Order and Solid-State Structure in Organic Field-Effect Transistors. *Chem. Rev.* **2011**, *111*, 4833−4856.

(4) Schweicher, G.; Olivier, Y.; Lemaur, V.; Geerts, Y. H. What Currently Limits Charge Carrier Mobility in Crystals of Molecular Semiconductors? *Isr. J. Chem.* **2014**, *54*, 595−620.

(5) Wang, C.; Dong, H.; Hu, W.; Liu, Y.; Zhu, D. Semiconducting π-Conjugated Systems in Field-Effect Transistors: A Material Odyssey of Organic Electronics. *Chem. Rev.* **2012**, *112*, 2208−2267.

(6) Bouchoms, I. P. M.; Schoonveld, W. A.; Vrijmoeth, J.; Klapwijk, T. M. Morphology Identification of the Thin Film Phases of Vacuum Evaporated Pentacene on SiO$_2$ Substrates. *Synth. Met.* **1999**, *104*, 175−178.

(7) Mattheus, C. C.; Dros, A. B.; Baas, J.; Oostergetel, G. T.; Meetsma, A.; de Boer, J. L.; Palstra, T. T. M. Identification of Polymorphs of Pentacene. *Synth. Met.* **2003**, *138*, 475−481.

(8) Fritz, S. E.; Martin, S. M.; Frisbie, C. D.; Ward, M. D.; Toney, M. F. Structural Characterization of a Pentacene Monolayer on an Amorphous SiO$_2$ Substrate with Grazing Incidence X-ray Diffraction. *J. Am. Chem. Soc.* **2004**, *126*, 4084−4085.

(9) Nabok, D.; Puschnig, P.; Ambrosch-Draxl, C.; Werzer, O.; Resel, R.; Smilgies, D.-M. Crystal and Electronic Structures of Pentacene Thin Films from Grazing-Incidence X-Ray Diffraction and First-Principles Calculations. *Phys. Rev. B* **2007**, *76*, 235322.

(10) Yoshida, H.; Inaba, K.; Sato, N. X-Ray Diffraction Reciprocal Space Mapping Study of the Thin Film Phase of Pentacene. *Appl. Phys. Lett.* **2007**, *90*, 181930.

(11) Schiefer, S.; Huth, M.; Dobrinevski, A.; Nickel, B. Determination of the Crystal Structure of Substrate-Induced Pentacene Polymorphs in Fiber Structured Thin Films. *J. Am. Chem. Soc.* **2007**, *129*, 10316−10317.

(12) Yoshida, H.; Sato, N. Crystallographic and Electronic Structures of Three Different Polymorphs of Pentacene. *Phys. Rev. B* **2008**, *77*, 235205.

(13) Mannsfeld, S. C. B.; Virkar, A.; Reese, C.; Toney, M. F.; Bao, Z. Precise Structure of Pentacene Monolayers on Amorphous Silicon Oxide and Relation to Charge Transport. *Adv. Mater.* **2009**, *21*, 2294−2298.

(14) Wedl, B.; Resel, R.; Leising, G.; Kunert, B.; Salzmann, I.; Oehzelt, M.; Koch, N.; Vollmer, A.; Duhm, S.; Werzer, O.; Gbabode, G.; Sferrazza, M.; Geerts, Y. Crystallisation Kinetics in Thin Films of Dihexyl-Terthiophene: The Appearance of Polymorphic Phases. *RSC Adv.* **2012**, *2*, 4404−4414.

(15) Werzer, O.; Boucher, N.; de Silva, J. P.; Gbabode, G.; Geerts, Y. H.; Konovalov, O.; Moser, A.; Novak, J.; Resel, R.; Sferrazza, M. Interface Induced Crystal Structures of Dioctyl-Terthiophene Thin Films. *Langmuir* **2012**, *28*, 8530−8536.

(16) Giri, G.; Verploegen, E.; Mannsfeld, S. C. B.; Atahan-Evrenk, S.; Kim, D. H.; Lee, S. Y.; Becerril, H. A.; Aspuru-Guzik, A.; Toney, M. F.; Bao, Z. Tuning Charge Transport in Solution-Sheared Organic Semiconductors Using Lattice Strain. *Nature* **2011**, *480*, 504−508.

(17) Salzmann, I.; Nabok, D.; Oehzelt, M.; Duhm, S.; Moser, A.; Heimel, G.; Puschnig, P.; Ambrosch-Draxl, C.; Rabe, J. P.; Koch, N. Structure Solution of the 6,13-Pentacenequinone Surface-Induced Polymorph by Combining X-Ray Diffraction Reciprocal-Space Mapping and Theoretical Structure Modeling. *Cryst. Growth Des.* **2011**, *11*, 600−606.

(18) Gbabode, G.; Dumont, N.; Quist, F.; Schweicher, G.; Moser, A.; Viville, P.; Lazzaroni, R.; Geerts, Y. H. Substrate-Induced Crystal Plastic Phase of a Discotic Liquid Crystal. *Adv. Mater.* **2012**, *24*, 658−662.

(19) Lercher, C.; Resel, R.; Balandier, J.-Y.; Niebel, C.; Geerts, Y. H.; Sferrazza, M.; Gbabode, G. Effects of Temperature on the Polymorphism of α,ω-Dioctylterthiophene in Thin Films. *J. Cryst. Growth* **2014**, *386*, 128−134.

(20) Chattopadhyay, B.; Ruzié, C.; Resel, R.; Henri Geerts, Y. Substrate-Induced Phases: Transition from a Liquid-Crystalline to a Plastic Crystalline Phase via Nucleation Initiated by the Substrate. *Liq. Cryst.* **2014**, *41*, 302−309.

(21) Della Valle, R. G.; Venuti, E.; Brillante, A.; Girlando, A. Molecular Dynamics Simulations for a Pentacene Monolayer on Amorphous Silica. *ChemPhysChem* **2009**, *10*, 1783−1788.

(22) Yoneya, M.; Kawasaki, M.; Ando, M. Molecular Dynamics Simulations of Pentacene Thin Films: The Effect of Surface on Polymorph Selection. *J. Mater. Chem.* **2010**, *20*, 10397−10402.

(23) Drummy, L. F.; Martin, D. C. Thickness-Driven Orthorhombic to Triclinic Phase Transformation in Pentacene Thin Films. *Adv. Mater.* **2005**, *17*, 903−907.

(24) Cheng, H.-L.; Mai, Y.-S.; Chou, W.-Y.; Chang, L.-R.; Liang, X.-W. Thickness-Dependent Structural Evolutions and Growth Models in Relation to Carrier Transport Properties in Polycrystalline Pentacene Thin Films. *Adv. Funct. Mater.* **2007**, *17*, 3639−3649.

(25) Knipp, D.; Street, R. A.; Völkel, A.; Ho, J. Pentacene Thin Film Transistors on Inorganic Dielectrics: Morphology, Structural Properties, and Electronic Transport. *J. Appl. Phys.* **2003**, *93*, 347−355.

(26) Dickey, K. C.; Anthony, J. E.; Loo, Y.-L. Improving Organic Thin-Film Transistor Performance through Solvent-Vapor Annealing of Solution-Processable Triethylsilylethynyl Anthradithiophene. *Adv. Mater.* **2006**, *18*, 1721−1726.

(27) Palermo, V.; Samorì, P. Molecular Self-Assembly across Multiple Length Scales. *Angew. Chem., Int. Ed.* **2007**, *46*, 4428−4432.

(28) Luca, G. D.; Treossi, E.; Liscio, A.; Mativetsky, J. M.; Scolaro, L. M.; Palermo, V.; Samorì, P. Solvent Vapour Annealing of Organic Thin Films: Controlling the Self-Assembly of Functional Systems across Multiple Length Scales. *J. Mater. Chem.* **2010**, *20*, 2493−2498.

(29) Zhao, Y.; Xie, Z.; Qu, Y.; Geng, Y.; Wang, L. Solvent-Vapor Treatment Induced Performance Enhancement of poly(3-Hexylthiophene):methanofullerene Bulk-Heterojunction Photovoltaic Cells. *Appl. Phys. Lett.* **2007**, *90*, 043504.

(30) Amassian, A.; Pozdin, V. A.; Li, R.; Smilgies, D.-M.; Malliaras, G. G. Solvent Vapor Annealing of an Insoluble Molecular Semiconductor. *J. Mater. Chem.* **2010**, *20*, 2623−2629.

(31) Moser, A.; Novák, J.; Flesch, H.-G.; Djuric, T.; Werzer, O.; Haase, A.; Resel, R. Temperature Stability of the Pentacene Thin-Film Phase. *Appl. Phys. Lett.* **2011**, *99*, 221911.

(32) Ebata, H.; Izawa, T.; Miyazaki, E.; Takimiya, K.; Ikeda, M.; Kuwabara, H.; Yui, T. Highly Soluble [1]Benzothieno[3,2-B]-benzothiophene (BTBT) Derivatives for High-Performance, Solution-Processed Organic Field-Effect Transistors. *J. Am. Chem. Soc.* **2007**, *129*, 15732−15733.

(33) Izawa, T.; Miyazaki, E.; Takimiya, K. Molecular Ordering of High-Performance Soluble Molecular Semiconductors and Re-Evaluation of Their Field-Effect Transistor Characteristics. *Adv. Mater.* **2008**, *20*, 3388−3392.

(34) Liu, C.; Minari, T.; Lu, X.; Kumatani, A.; Takimiya, K.; Tsukagoshi, K. Solution-Processable Organic Single Crystals with

Bandlike Transport in Field-Effect Transistors. *Adv. Mater.* **2011**, *23*, 523−526.

(35) Minemawari, H.; Yamada, T.; Matsui, H.; Tsutsumi, J.; Haas, S.; Chiba, R.; Kumai, R.; Hasegawa, T. Inkjet Printing of Single-Crystal Films. *Nature* **2011**, *475*, 364−367.

(36) Amin, A. Y.; Reuter, K.; Meyer-Friedrichsen, T.; Halik, M. Interface Engineering in High-Performance Low-Voltage Organic Thin-Film Transistors Based on 2,7-Dialkyl-[1]benzothieno[3,2-b][1]benzothiophenes. *Langmuir* **2011**, *27*, 15340−15344.

(37) Amin, A. Y.; Khassanov, A.; Reuter, K.; Meyer-Friedrichsen, T.; Halik, M. Low-Voltage Organic Field Effect Transistors with a 2-Tridecyl[1]benzothieno[3,2-b][1]benzothiophene Semiconductor Layer. *J. Am. Chem. Soc.* **2012**, *134*, 16548−16550.

(38) Colella, S.; Ruzié, C.; Schweicher, G.; Arlin, J.-B.; Karpinska, J.; Geerts, Y.; Samorì, P. High Mobility in Solution-Processed 2,7-Dialkyl-[1]benzothieno[3,2-b][1]benzothiophene-Based Field-Effect Transistors Prepared with a Simplified Deposition Method. *ChemPlusChem.* **2014**, *79*, 371−374.

(39) Yuan, Y.; Giri, G.; Ayzner, A. L.; Zoombelt, A. P.; Mannsfeld, S. C. B.; Chen, J.; Nordlund, D.; Toney, M. F.; Huang, J.; Bao, Z. Ultra-High Mobility Transparent Organic Thin Film Transistors Grown by an off-Centre Spin-Coating Method. *Nat. Commun.* **2014**, *5*, 3005.

(40) Elemans, J. A. A. W.; Lei, S.; De Feyter, S. Molecular and Supramolecular Networks on Surfaces: From Two-Dimensional Crystal Engineering to Reactivity. *Angew. Chem., Int. Ed.* **2009**, *48*, 7298−7332.

(41) Sheldrick, G. M. A Short History of *SHELX*. *Acta Crystallogr., Sect. A* **2008**, *64*, 112−122.

(42) Nečas, D.; Klapetek, P. Gwyddion: An Open-Source Software for SPM Data Analysis. *Cent. Eur. J. Phys.* **2012**, *10*, 181−188.

(43) Rubio-Zuazo, J.; Ferrer, P.; López, A.; Gutiérrez-León, A.; da Silva, I.; Castro, G. R. The Multipurpose X-Ray Diffraction End-Station of the BM25B-SpLine Synchrotron Beamline at the ESRF. *Nucl. Instrum. Methods Phys. Res., Sect. A* **2013**, *716*, 23−28.

(44) Ferrer, P.; Rubio-Zuazo, J.; Heyman, C.; Esteban-Betegón, F.; Castro, G. R. Multi-Use High/low-Temperature and Pressure Compatible Portable Chamber for *in Situ* Grazing-Incidence X-Ray Scattering Studies. *J. Synchrotron Radiat.* **2013**, *20*, 474−481.

(45) Moser, A. Crystal Structure Solution Based on Grazing Incidence X-ray Diffraction: Software Development and Application to Organic Films. *Ph.D. Thesis*, Graz University of Technology, Graz, Austria, 2012.

(46) Erko, A.; Packe, I.; Hellwig, C.; Fieber-Erdmann, M.; Pawlizki, O.; Veldkamp, M.; Gudat, W. KMC-2: The New X-Ray Beamline at BESSY II. In *AIP Conference Proceedings*; AIP Publishing: Melville, NY, 2000; Vol. *521*, pp 415−418.

(47) Kriegner, D.; Wintersberger, E.; Stangl, J. *xrayutilities*: A Versatile Tool for Reciprocal Space Conversion of Scattering Data Recorded with Linear and Area Detectors. *J. Appl. Crystallogr.* **2013**, *46*, 1162−1170.

(48) Hlawacek, G.; Teichert, C. Nucleation and Growth of Thin Films of Rod-like Conjugated Molecules. *J. Phys.: Condens. Matter* **2013**, *25*, 143202.

(49) Werzer, O.; Stadlober, B.; Haase, A.; Oehzelt, M.; Resel, R. Full X-Ray Pattern Analysis of Vacuum Deposited Pentacene Thin Films. *Eur. Phys. J. B* **2008**, *66*, 455−459.

(50) Burger, A.; Ramberger, R. On the Polymorphism of Pharmaceuticals and Other Molecular Crystals. II. *Microchim. Acta* **1979**, *72*, 273−316.